Iranian Journal of Electrical and Electronic Engineering 03 (2020) 313–324
Special Issue on Smart Grids

Iranian Journal of Electrical and Electronic Engineering

Journal Homepage: ijeee.iust.ac.ir

Research Paper

Improvement of Transient Voltage Profile Using Power Control of the DFIG-Based Wind Farm Under Severe Voltage Dip Event

Z. Rafiee*, M. Rafiee*, and M. R. Aghamohammadi*(C.A.)

Abstract: Improving transient voltage stability is one of the most important issues that must be provided by doubly fed induction generator (DFIG)-based wind farms (WFs) according to the grid code requirement. This paper proposes adjusted DC-link chopper based passive voltage compensator and modified transient voltage controller (MTVC) based active voltage compensator for improving transient voltage stability. MTVC is a controller-based approach, in which by following a voltage dip (VD) condition, the voltage stability for the WF can be improved. In this approach, a voltage dip index (VDI) is proposed to activate/deactivate the control strategy, in which, two threshold values are used. In the active mode, the active and reactive power are changed to decrease the rotor current and boost the PCC voltage, respectively. Based on the control strategy, in a faulty grid, DFIG not only will be able to smooth DC-link voltage fluctuations and reduces rotor overcurrents but also it will increase the voltage of point of common coupling (PCC). Therefore, it improves transient voltage stability. The simulation results show the effectiveness of the proposed strategy for improving voltage stability in the DFIG.

Keywords: Doubly Fed Induction Generator (DFIG), Imperialist Competitive Algorithm (ICA), Transient Voltage Stability, Voltage Dip.

1 Introduction

WITH the wide integration of renewable energy sources, wind energy has gained popularity as an electrical energy source in many countries. This wind energy through the wind turbines and then WFs is converted to electrical energy. As, 5.5% of the world's electricity needs are supplied by wind power plants in 2018 [1] and at the end of 2018, WF capacity connected to the grid in the world has reached 596.6GW [2]. In WFs, DFIG are widely utilized due to their capability for decoupled control of active and reactive powers, high efficiency, lightweight, and good speed control [3].

Iranian Journal of Electrical and Electronic Engineering, 2020.
Paper first received 25 September 2019, revised 12 February 2020, and accepted 13 February 2020.
* The authors are with the Faculty of Electrical Engineering, Shahid Beheshti University, Daneshju Blvd, Velenjak, Tehran, 1983969411, Iran.
E-mails: z_rafiee@sbu.ac.ir, m_rafiee@sbu.ac.ir, and m_aghamohammadi@sbu.ac.ir.
Corresponding Author: M. R. Aghamohammadi.

WFs can affect on the voltage, frequency, stability and security of the grid [4, 5]. Therefore, disconnecting of large WFs may cause system instability in the following of a VD [6]. Hence, to achieve the efficient grid voltage support in a faulty grid, transient voltage at the PCC should satisfy the specified limit voltage-time curves. WFs also require reactive power support as to meet grid code requirements [7].

However, DFIG-WF is vulnerable to change the PCC voltage causing DC-link overvoltage and rotor overcurrent in VD conditions [8, 9]. These phenomena can damage the rotor side converter (RSC) of the DFIG and cause the WF to trip from the grid due to the lack of transient voltage stability [10]. So, WF must remain connected to the grid during a VD condition for improving voltage stability [11]. In addition, immediately after VD clearance, WFs must be able to provide active power for maintaining grid stability. In order to remain the DFIG-WF connected to the grid for supporting the grid voltage in a VD conditions, various strategies have been proposed which can be classified in three categories:

1. Device-based approaches: these approaches need extra hardware such as energy storage devices, FACTS devices, fault current limiter, and other devices.
2. Controller-based approaches: by utilizing these approaches, back to back converter are specially controlled using advanced and classic methods in which terms are added to controlling signal.
3. Device and controller-based approaches: in these methods, extra hardware and special control of back to back converter are simultaneously applied.

In the meantime, crowbar resistance and DC-link chopper are only used for protecting electronic devices during severe VD conditions which cause to disconnect the DFIG-WF to the grid. By connecting the crowbar resistance, DFIG is converted to squirrel cage induction generator causing the loose of controllability and absorption more reactive power from the grid and thus, more decrease of the PCC voltage happens [12]. DC-chopper in parallel with the capacitor at the DC-link is another device for protecting DC-link against overvoltage [13]. There are other device-based approaches trying to improve LVRT capability namely STATCOM adopted as parallel reactive power source connected between the grid and WF [14], dynamic voltage restorer (DVR) in series with WF and grid as series injecting reactive power [15, 16] normally employed to compensate the reduced voltage at the PCC but these devices increase the complexity and unreliability of the WF systems. Super capacitor energy storage system (ESS) connected to the WF bus proposed in [17], limits fault current on the DFIG while the transient voltage stability improvement might be degraded on severe VDs. Series dynamic braking resistors (SDBRs) in series with the rotor limits high rotor current but it has not the ability to increase the grid voltage. however, SDBRs are large and complex [18] and need power electronic devices which are not safe. SDBRs in series with the stator [19] can improve the post-fault recovery and, hence, the transient stability of the DFIG- WF. Therefore, eliminates the need for using complicated reactive power compensator devices. However, SDBR does not the ability to hold the voltage profile ±0.1 p.u. of nominal value, its ability to stabilize the DC voltage is poor [20]. Also, it produces huge amount of harmonics into the system. bridge type fault current limiter connected to the DFIG-WF and grid [21], DC-link switchable resistive-type fault current limiter (SRFCL) [22], [23], and saturated core fault current limiter [24] are proposed for decreasing the harmful effects of the VD and increase the PCC voltage. FCLs can improve transient voltage stability better than the other approach [20] but they have adverse effects on the system stability and LVRT performance during the post-fault stage [25]. Also, a sole FCL cannot provide any reactive power for efficient voltage support. Moreover, SFCL is very costly due to its superconductivity nature. However, using device-based strategies need extra hardware devices resulting in cost increase and reliability reduction for DFIG. In order to overcome the drawbacks of the device-based approaches, researchers often propose controller and device-based approaches. Controller-based approach such as reverse current tracking in which the rotor current references are determined based on the stator currents [26], Modified feed-forward compensators [27] hybrid method based on the multi-objective algorithm of krill and the fuzzy controller [28], and GA-Based Optimal LQR Controller [29] can only decrease rotor overcurrent and DC-link overvoltage in the VD conditions. one of the controller-based approach is the control of the DFIG converters regulators to take part in the transient voltage control (TVC) [30] but its available reactive power is inadequate to support the PCC voltage due to severe VD conditions.

Therefore, a modified TVC is proposed in this paper to support PCC voltage during severe VD condition. By using the proposed method, the voltage stability in DFIG-WF can be improved following a VD event. In this approach, a voltage index as VDI is proposed to activate/deactivate the control strategy, in which two threshold values α and β are used. In the active mode, the active and reactive power are changed to zero and one p.u for decreasing the rotor current and boost the PCC voltage, respectively. According to the grid requirements, in the deactivate mode, they are changed to one and zero p.u, respectively. Based on the proposed control strategy, during a VD condition, DFIG will be able to smooth DC link voltage fluctuations and significantly reduces the of the stator and rotor overcurrent.

Furthermore, the direct power control (DPC) method is modified to adaptively change the rotor current reference values based on the severity of VD. The parameters of the PI controllers are tuned by the imperialist competitive algorithm (ICA) using the sum of the sample values in the discrete Fourier transform (SMVS-DFT) for evaluating the objective function. The major novelties of the proposed approach are as follows.

1. Compared to the conventional controller-based strategies, the suggested scheme can compensate for the voltage of the PCC and improves transient voltage stability compared to the literature.
2. The simulation results of the proposed method show that the approach is able to decrease rotor overcurrent and DC-link overvoltage.
3. Contrary to the classical approaches, active and reactive power sharing are maintained during both steady state and transients. Finally, the simulation results show the effectiveness of the proposed control strategy for improving the transient voltage stability of DFIG.

This paper is organized as follows. DFIG modeling and transient behaviors of DFIG are analytically

investigated in Section 2. In Section 3, the principle of the proposed control strategy has been expressed. The proposed strategy of DFIG is presented in Section 4. The imperialist competition algorithm is presented in Section 5. In Section 6, the feasibility and effectiveness of the proposed control strategy are validated in MATLAB/Simulink environment.

2 DFIG Under Grid Fault

2.1 DFIG Model

In this study, DFIG is modeled by the detailed dynamic model using the following voltage equations specified in the synchronous reference frame [31]:

The flux equations can be shown as:

$$\begin{cases} \dfrac{d\lambda_s}{dt} = u_s - R_s i_s - j\omega_e \lambda_s \\ \dfrac{d\lambda_r}{dt} = u_r - R_r i_r - j(\omega_e - \omega_r)\lambda_r \end{cases} \quad (1)$$

By i_s and i_r, the state space equations can be derived as (2). State space equations of the DFIG can be used to check the DFIG behavior in the of various fault events in the grid. Finally, the state space equations of the DFIG in the synchronous reference can be expressed as (3).

2.2 The Transient Behaviors of DFIG

DFIG is highly sensitive to change the PCC voltage. Generally, when a fault occurs in the grid causing a VD at the PCC of the DFIG, if the necessary actions are not taken, the following problems can arise:

- Stator flux oscillations;
- Increase of the electromagnetic force in the rotor winding;
- Increase of the rotor current;
- Increase of the DC link voltage;
- Swing in torque and speed.

By reducing the PCC voltage of DFIG, the stator flux varies and large electromagnetic force (about 3 to 4 times the nominal value) is induced in the rotor winding [32]. This phenomenon can be explained as follows:

Rotor voltage in stator reference frame can be expressed as:

$$u_r^s = R_r i_r^s + \frac{d\lambda_r^s}{dt} = \underbrace{\frac{L_m}{L_s}\frac{d\lambda_s^s}{dt}}_{EMF_r^s} + \left(R_r + \sigma L_r \frac{d}{dt}\right) i_r^s \quad (4)$$

where $(1\text{-}L_m^2/(L_sL_r))$ is rotor leakage coefficient (σ_r). In (4), the first term refers to the induced voltage in the rotor winding due to the stator flux fluctuations which is denoted as EMF_r^s (induced electric magnetic force in rotor in the stator reference frame). EMF_r^s in rotor reference frame can be expressed as in normal condition:

$$EMF_r^r = \frac{L_m}{L_s}\frac{d\lambda_s^r}{dt} = \frac{L_m}{L_s} s U_s e^{j\omega_s t} \quad (5)$$

where $\omega_s = s\omega_e = \omega_e - \omega_r$. Generally, at normal conditions, slip (s) varies between -0.3 and +0.3 yielding a low value for EMF_r^r. When the PCC voltage decreases due to a symmetrical fault in the grid, EMF_r^r in the rotor reference frame is expressed as follow [32, 33]:

$$\begin{aligned} EMF_r^r &= \frac{L_m}{L_s}\frac{d}{dt}\lambda_s^r \\ &= \frac{L_m}{L_s}\left[sU_s(1-g)e^{j(\omega_e-\omega_r)t} - \frac{U_s g}{j\omega_e}\left(\frac{1}{\tau_s} + j\omega_r\right)e^{-j\omega_r t_e - t/\tau_s}\right] \end{aligned} \quad (6)$$

where $\tau_s = L_s / R_s$ is the time constant of the stator winding and g refers to the VD percentage. By neglecting $1/\tau_s$, (6) can be simplified as:

$$\begin{aligned} EMF_r^r = \frac{L_m}{L_s}\Big[& sU_s(1-g)e^{j(\omega_e-\omega_r)t} \\ & - U_s g(1-s)e^{-j\omega_r t_e - t/\tau_s}\Big] \end{aligned} \quad (7)$$

$$\begin{cases} \dfrac{d\lambda_s}{dt} = u_s - R_s\left(\dfrac{L_r}{L_{ls}L_{lr}+L_{ls}L_m+L_{lr}L_m}\times\lambda_s - \dfrac{L_m}{L_{ls}L_{lr}+L_{ls}L_m+L_{lr}L_m}\times\lambda_r\right) - j\omega_e\lambda_s \\ \dfrac{d\lambda_r}{dt} = u_r - R_r\left(\dfrac{-L_m}{L_{ls}L_{lr}+L_{ls}L_m+L_{lr}L_m}\times\lambda_s + \dfrac{L_s}{L_{ls}L_{lr}+L_{ls}L_m+L_{lr}L_m}\times\lambda_r\right) - j(\omega_e-\omega_r)\lambda_r \end{cases} \quad (2)$$

$$\begin{cases} \dfrac{d\lambda_{sd}}{dt} = u_{sd} - R_s\left(\dfrac{L_r}{L_{ls}L_{lr}+L_{ls}L_m+L_{lr}L_m}\times\lambda_{sd} - \dfrac{L_m}{L_{ls}L_{lr}+L_{ls}L_m+L_{lr}L_m}\times\lambda_{rd}\right) + j\omega_e\lambda_{sq} \\ \dfrac{d\lambda_{sq}}{dt} = u_{sq} - R_s\left(\dfrac{L_r}{L_{ls}L_{lr}+L_{ls}L_m+L_{lr}L_m}\times\lambda_{sq} - \dfrac{L_m}{L_{ls}L_{lr}+L_{ls}L_m+L_{lr}L_m}\times\lambda_{rq}\right) - j\omega_e\lambda_{sd} \\ \dfrac{d\lambda_{rd}}{dt} = u_{rd} - R_r\left(\dfrac{-L_m}{L_{ls}L_{lr}+L_{ls}L_m+L_{lr}L_m}\times\lambda_{sd} + \dfrac{L_s}{L_{ls}L_{lr}+L_{ls}L_m+L_{lr}L_m}\times\lambda_{rd}\right) + j(\omega_e-\omega_r)\lambda_{rq} \\ \dfrac{d\lambda_{rq}}{dt} = u_{rq} - R_r\left(\dfrac{-L_m}{L_{ls}L_{lr}+L_{ls}L_m+L_{lr}L_m}\times\lambda_{sq} + \dfrac{L_s}{L_{ls}L_{lr}+L_{ls}L_m+L_{lr}L_m}\times\lambda_{rq}\right) - j(\omega_e-\omega_r)\lambda_{rd} \end{cases} \quad (3)$$

From (7), it can be illustrated that at the initial moments of the fault event (t = 0), the induced EMF_r^r (0) is relatively large due to the DC offset in the flux. For example, for s = –0.2 and g = 1, the value of the EMF_r^r (0) becomes $(1.2U_sL_m)/L_s$ in the initial moments, which is 6 times the normal value.

3 Principle of the Proposed Control Method

In this section, the principle of the proposed controller-based approach for enhancing transient voltage stability is explained. Improving the transient voltage stability along with the mitigation of rotor overcurrent and increase of PCC voltage are achieved by modified TVC, in which active and reactive power reference values change by following VD.

Fig. 1 shows the conventional TVC. This method determines the values of rotor voltage and GSC voltage in synchronous reference frame. GSC voltage tunes output reactive power of DFIG and DC-link voltage. Rotor voltage also specifies the output active and reactive power of DFIG-based wind turbine. In conventional TVC method, in order to transient voltage control, reactive power reference in RSC and GSC that it is utilized the q-axis rotor voltage and GSC voltage is determined by error between measured voltage and voltage reference of the PCC and thus, this error determines the q-axis rotor current and GSC current references. In proposed modified TVC, active and reactive power references change in the following of VD. In this method active power reference also changes under VD condition compare to the conventional TVC in which active power doesn't change. This change causes not increase the rotor current due to the increase of reactive power. Furthermore, under severe VD, DFIG-based wind turbine injects the whole reactive power that can generated to the grid. It causes that DFIG acts similar to reactive compensator devices and thus, it prevents instability of grid and increases transient voltage stability which threatened by VD. On the other hand, adjusted DC-link chopper as passive voltage compensator makes to generate reactive power in VD condition and increase the transient voltage stability.

3.1 Control of the Rotor Current by Active Power Reference Value

Using space vector control, the stator voltage vector u_s is orientated with the d-axis grid voltage. As a result, the dq-axis grid voltage will be as follows [34]:

$$u_{qs} = 0 \quad \Rightarrow \quad u_{ds} = \sqrt{u_s^2 - u_{qs}^2} = u_s \tag{8}$$

Applying vector control strategy for DFIG, the dq-axis rotor currents can be evaluated as follows:

$$i_{dr} = -\left(\frac{2L_s}{3u_{ds}L_m}\right)P_s - \left(\frac{R_s}{\omega_e L_m}\right)i_{qs} \tag{9}$$

$$i_{qr} = \left(\frac{2L_s}{3u_{ds}L_m}\right)Q_s + \left(\frac{R_s}{\omega_e L_m}\right)i_{ds} - \left(\frac{1}{\omega_e L_m}\right)u_{ds} \tag{10}$$

By neglecting resistance of the stator winding in (9) and (10), the following can be obtained:

$$i_{dr} = -\left(\frac{2L_s}{3u_{ds}L_m}\right)P_s \tag{11}$$

$$i_{qr} = \left(\frac{2L_s}{3u_{ds}L_m}\right)Q_s - \left(\frac{1}{\omega_e L_m}\right)u_{ds} \tag{12}$$

As can be seen in (11) and (12), the behavior of i_{dr} and i_{qr} are decoupled and i_{dr} is directly proportional to P_s and i_{qr} is directly related to Q_s. Therefore, by changing

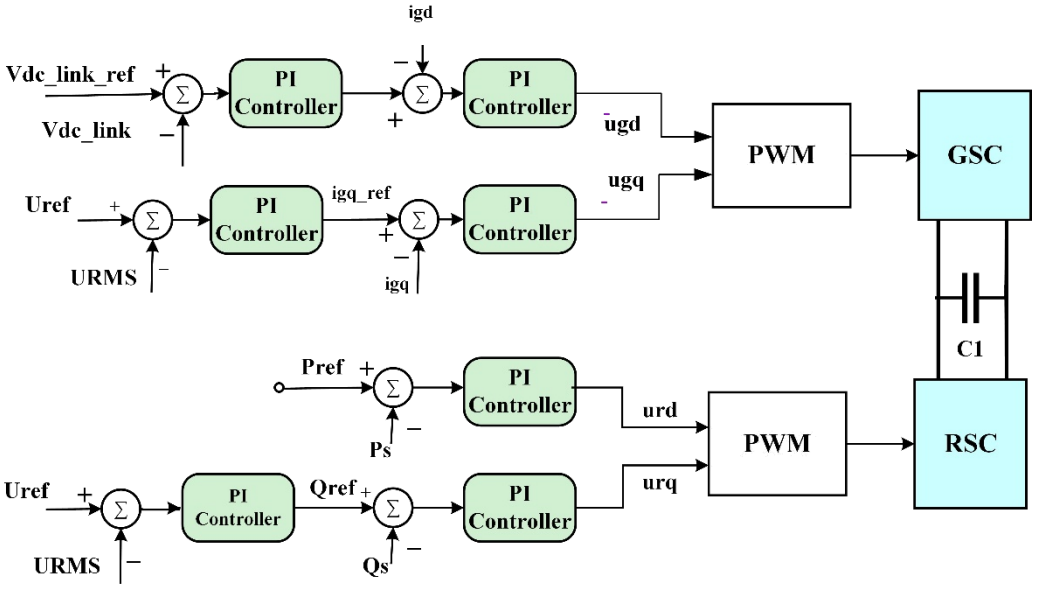

Fig. 1 Conventional transient voltage control.

the active and reactive power references, the dq-axis rotor currents can be controlled. As a result of the proposed control method, during a VD event when active power reference value changes to a lower value, idr will decrease causing reduction of the rotor current.

3.2 Control of the PCC Voltage by Reactive Power Reference Value

Using two-bus system shown in Fig. 2(a), the relationship between voltage V2 and reactive power *Q* can be derived. According to the corresponding phasor diagram shown in Fig. 2(b), the following equations can be obtained:

$$(U1-U2)^2 = \Delta U^2 = \Delta U_R^2 + \Delta U_X^2 = (RI\cos\varphi + XI\sin\varphi)^2 + (XI\cos\varphi - RI\sin\varphi)^2 \quad (13)$$

Neglecting ΔU_X compared to ΔU_R because ΔU_X influence on the phase more, the voltage drop can be obtained with respect to P_2 and Q_2.

$$\Delta U = RI\cos\varphi + XI\sin\varphi \quad (14)$$

Since $R << X$, the voltage drop caused by the resistor can be ignored, thus (14) can be written as follow:

$$\Delta U \simeq XI\sin\varphi \quad (15)$$

So

$$\Delta U = \frac{XIU_2\sin\varphi}{U_2} = \frac{XQ_2}{U_2} \text{ or } Q_2 = \frac{U_2}{X}\Delta U \quad (16)$$

where Q_2 is reactive power *R* and *X*, U_2 and U_1 are voltage buses, and *I* is current line. Equation (15) can be rewritten as follows.

$$U_2 = \frac{X}{\Delta U}Q_2 \quad (17)$$

Therefore, it can be concluded that the voltage is mainly dominated by the reactive power. Therefore, during a VD event for increasing the voltage of the PCC, it can be sufficient to increase the reactive power reference value.

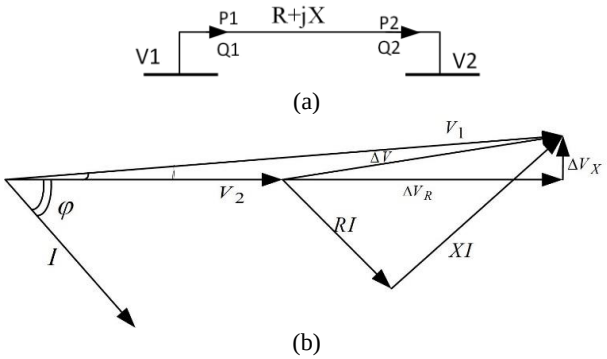

Fig. 2 a) Two-bus system and b) voltage phasor diagram.

3.3 Decision Algorithm for Changing Reference Values in Modified TVC

In the previous sections, it is shown that by changing active and reactive power of DFIG, it is able to control the rotor current and the PCC voltage. According to this fact, in the proposed modified TVC, during a VD event in order to reduce rotor current and increase PCC voltage, active and reactive powers of DFIG should be decreased and increased respectively. For this purpose, immediately following detection of a VD event, the reactive and active power reference values should be set to one and zero, respectively to support network voltage and avoid rotor over current. Fig. 3 shows the decision algorithm to activate and deactivate the control strategy when a VD occurs. At each time instant, the measured VRMS is compared with the voltage reference value (1 p.u.) from which voltage dip index (VDI) is calculated. According to the decision algorithm shown in Fig. 3, for VDI(t) $\geq \alpha$, active and reactive power reference values are set to 0 and 1 respectively. Once VDI(t) gets smaller than β, the reference values are returned to the normal setting.

4 Proposed Control Strategy

In this paper, based on the changing active and reactive power reference values and using MDPC, a new control strategy is proposed to increase the PCC voltage and suppress the DC-link voltage and rotor current resulting in LVRT capability enhancement. The key issue in the proposed control approach is the increase of the PCC voltage using a controller-based approach during a VD event. MDPC is used for fast regulation of DFIG output powers. The proposed MDPC is a hybrid mix of direct power and vector control methods, in which based on the vector control theory, the generator terminal voltage aligns with the d-axis of the synchronous reference frame. Fig. 4 shows the structure of the proposed control strategy. As it can be seen, the on-off hysteresis controllers of DPC are replaced with PI controllers. Similar to the DPC strategy, the input signals of the PI controllers are the stator output powers error vectors, used to build rotor voltage. The built rotor voltage is given to pulse width modulation unit (PWM) to create switching signals for RSC. By the proposed approach, following a VD, the following capabilities for LVRT of DFIG could be provided:

1. Ensuring that DFIG can stay connected to the grid during a VD event by effectively decreasing the stator and rotor currents as well as reducing the DC-link voltage.
2. Contributing to network voltage support by providing a reactive power in response to a VD at the PCC depending on the VD level of the PCC (e.g. 4% reactive power for 1% VD [35]).
3. Participating in the network frequency control by generating sufficient active power after the fault

clearance (e.g. larger or equal to 95% of the pre-fault active power in 100ms after fault clearance [27]).

In order to apply the proposed control strategy, first, it is necessary to tune PI controllers' parameters of DFIG as shown in Fig. 4. For this purpose, DFIG is modeled in the state space with six-controlled current sources and by using ICA optimization algorithm, the PI control parameters are tuned optimally. The ICA and SMVS-DFT as objective function is utilized to design PI controllers to control steady-state and transient behavior of DFIG. Then, by setting optimal PI controllers' parameters for DFIG (by tracking active and reactive power reference values) its steady state condition is evaluated.

The proposed control approach (modified TVC) is continuously performed within a moving time window with the length of 16/7ms (sample frequency/system frequency) including 34 samples which are gathered by a sampling rate of 20kHz using PMU. It is worth noting that the moving window is continuously updated for each sample (50μs). Fig. 5 shows the real time process of the proposed control strategy consisting of the following steps:

Step.1: At each moving time window for 34 samples provided by PMU by using discrete Fourier transform (DFT) the RMS value of the voltage magnitude at the terminal of DFIG is obtained.

Step.2: Using measured URMS, the VD index (VDI) is evaluated for activating/deactivating the proposed control strategy.

$$VDI(t) = 1.0 - U_{RMS}(t) \tag{18}$$

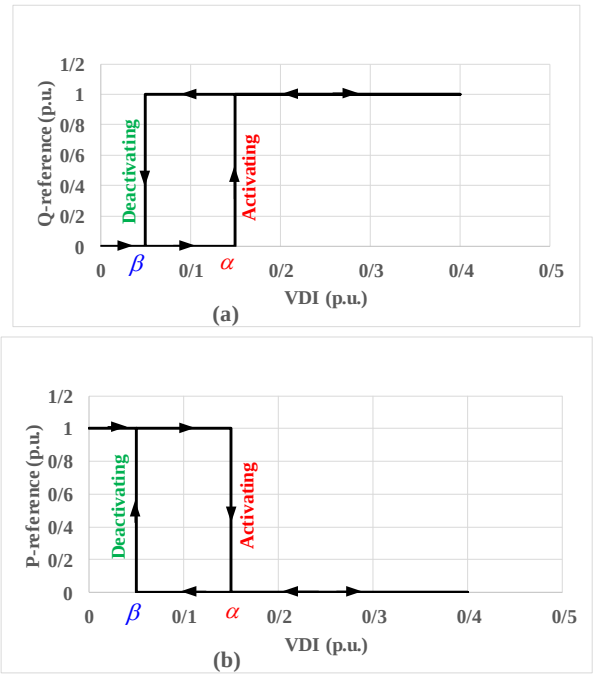

Fig. 3 Decision algorithm for changing active and reactive power references; a) reactive power and b) active power.

Step.3: The VD index (VDI) is compared to the threshold value α for activating the proposed control strategy.

If $VDI(t) > \alpha \rightarrow$ Active Control Strategy

Step.4: The VDI(t) is compared to the threshold value β for deactivating the proposed control strategy.

Step.5:

If $VDI(t) < \beta \rightarrow$ Deactive Control Strategy

As long as the VDI(t) remains between two threshold values (α > VDI(t) > β) the control strategy remains active.

It is worth noting that choosing proper values for α and β depend on the sensitivity of the voltage magnitude to reactive power compensation which is related to the short circuit capacity of the terminal of DFIG.

5 Imperialist Competition Algorithm

The Imperialist competition algorithm (ICA) has been chose for parameters optimization of PI controllers. This evolutionary optimization strategy has shown great performance in both convergence rate and better global optima achievement compared to particle swarm optimization and genetic algorithm. Nevertheless, its effectiveness, limitations and applicability in various domains are currently being extensively investigated [36]. Like other optimization algorithms, ICA starts with an initial population. Every population is a country which has two types: imperialists and colonies with together compose some empires. Imperialistic

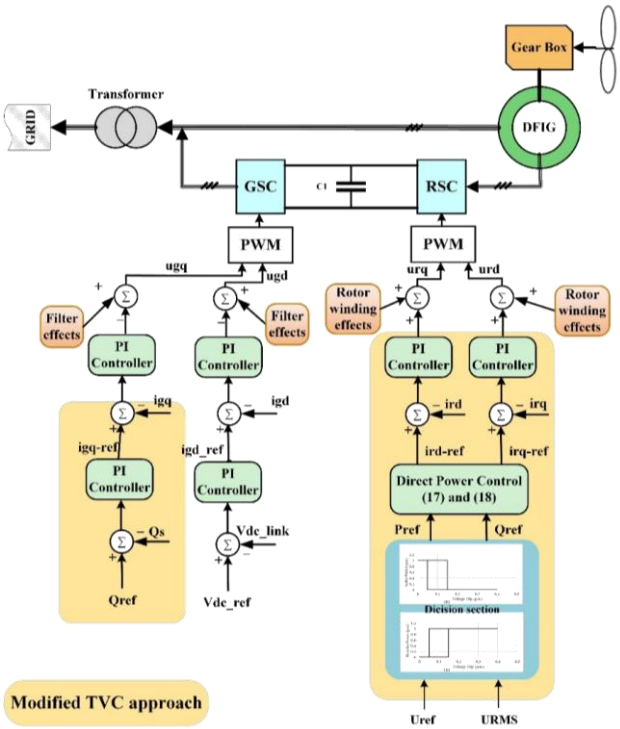

Fig. 4 Control diagram of proposed modified TVC.

competition among these empires forms the basis of the evolutionary algorithm. During the competition, powerful empires take possession of their colonies and weak empires collapse. Imperialistic competition hopefully converges to a state in which there exists only one empire and its colonies have the same cost as the imperialist and colonies are in the same position [36-38].

The objective function used in this approach is denoted as SMVS-DFT [37-39] which is composed of the deviation of active and reactive powers, DC link voltage, generator speed, and stator current with respect to their reference values. The weighting coefficients by which each variable can contribute in the objective function can be determined based on the empirical analysis of the variables deviation with respect to their reference values.

Initial number of countries is set at 100, 10 of which are chosen as the initial imperialists in the ICA. The maximum number of iterations (number of decades) of the ICA is set at 120 in which the objective function (SMVS-DFT) value using as follows:

$$OF = \sum_{k=1}^{(tstop\times f_s)} amplitude\left(\sum_{n=1}^{\infty}\left(25\Delta U_{DC}[n] + 10(\Delta P[n]+\Delta Q[n]) + 8\Delta\omega_r[n] + 30(\Delta i_{dr}[n]+\Delta i_{qr}[n])\right)e^{-jkn(2\pi f)}\right) \quad (19)$$

The optimized parameters are given in Table 1.

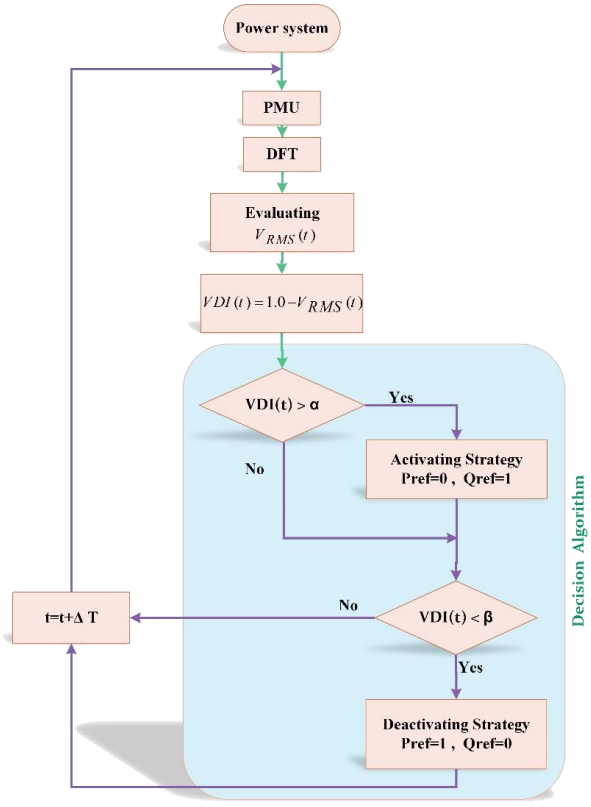

Fig. 5 Real time process of the proposed control strategy.

6 Simulation Results

In order to peruse the transient behavior of the DFIG during a VD condition, the following assumptions are considered:

1. DFIG operates in super-synchronous speed (slip = –0.2) with the potential of generating maximum rotor over current.
2. Wind speed variation is negligible, due to short duration of fault.
3. DFIG is operating at the steady state before VD condition.

The simulations were carried out using MATLAB/Simulink environment. A Three-phase voltage dip (3-phase Line to Ground) is applied on the grid as shown in Fig 6. Fig. 6 shows a grid-connected DFIG-WF system formed by 6 DFIG-based wind turbines 1.5MW with a superconducting fault current limiter (SFCL) installed between the Transformer T1 and Bus 690. The VD is applied at t = 1s. After 150ms, the VD is clear. For the analysis of transient voltage stability analysis, the wind speed is assumed constant at 15m/s. In order to show the effectiveness of the proposed modified TVC, the simulations are carried out for three following scenarios:

Scenario.A: Using conventional TVC approach for DFIG-based WF in a faulty grid,

Scenario.B: Using proposed modified TVC approach for DFIG-based WF.

Scenario.C: DFIG-based WF uses conventional TVC and superconducting fault current limiter (SFCL) [7].

Only using proposed SFCL approach for DFIG-based WF [7].

SFCL that used in Scenario C and D acts as follow: The symmetrical VD also causes serious stator overcurrent. When the stator overcurrent exceeds the critical current of the series connected SFCL, a self-acting SFCL impedance will boost suddenly to form a relatively large forward voltage drop across the SFCL and thus increase the stator voltage. This means that the SFCL is served as a passive stator voltage compensator [7].

Table 1 Parameters of PI controllers.

Element	Variable control	KP	KI
RSC	Active power	0.6	3
	Reactive power	0.6	3
GSC	DC-link voltage	5	200
		0.83	5
	Reactive power	0.5	30
		0.83	30

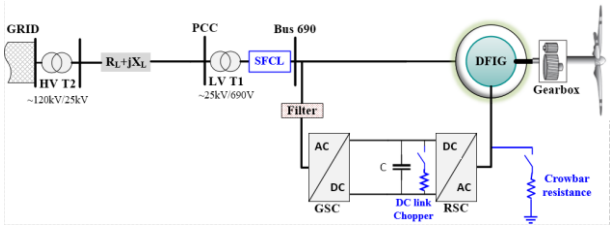

Fig. 6 System under study.

Figs. 7 and 8 show the DFIG-based WF behaviors for 0.7 p.u. VD and 0.9 p.u. VD as a severe VD event. Figs. 7(a) and 8(a) indicate the voltage profile at the PCC bus of the WF for Scenarios A and B. As depicted in these figures, in 0.9 VD event, using modified TVC, the increase of the PCC voltage is equal to 0.66 p.u while with applying the conventional TVC, this increase is equal to 0.33 p.u.. So, according to the results, the modified TVC has better performance in comparison with conventional TVC with lower voltage dip during fault compared with scenario A in both of VD conditions. So, in scenario B, the voltage recovery process is considerably short, which improves transient voltage as well in spite of this reality that the WF just injects 8MVar to the grid which leads to satisfy the grid code requirements. Figs. 7(b) and 8(b) represent the injected reactive power to the grid by the WF. As shown in Fig. 7(b), the injected reactive power to the grid is 2.53MVar during VD and 5.27MVar in the moment of VD event in scenario A, while these amounts are 8.01MVar during VD and 5.27MVar in the moment of VD event in scenario B. Also, in 0.9 p.u. VD event, the injected reactive power is 2.4 and 8MVar for using conventional and modified TVC approaches, respectively. It is clear that during VD event, the injected reactive power to the grid in the scenario B is higher than that in comparison with scenario A which effectively supports voltage profile at the PCC. Figs. 7(c) and 8(c) show the generated produced active power by the WF. In scenario B, the active power generated by the WF reaches to zero during fault, approximately causing the reduction of rotor over current during VD condition (the boost improvement of q-axis and the reduction of d-axis rotor current for the sake of the increase of the injected reactive power and decrease of the generated active power of the WF, respectively). Figs. 7(d) and 8(d) represent the DC link voltage of the DFIG for scenarios A and B. It is obvious that both conventional and modified TVC approaches effectively decrease the DC link over voltage. But, the modified TVC approach is more appropriate to decrease the oscillations than the conventional TVC, because it gives lower oscillation in 0.9 p.u. VD event as shown in Fig. 8(d). Figs. 7(e) and 8(e) display the DFIG rotor current for Scenarios A and B. As depicted in these figures, the rotor transient spike current is significantly limited and is lowest at the beginning and end of VD period in scenario B. Also, there is a remarkable decrease of the rotor current oscillations in scenario B particularly in 0.9 p.u. VD event. But, the modified TVC is more competent to do this than the conventional TVC because it gives lower oscillations and faster stabilization. As shown in Figs. 7(f) and 8(f), as a sequence of a decrease in active power, rotor speed is increased while it is significantly within the permissible range for two scenarios .The rate of rising of the DFIG speed is limited in both A and B scenarios, which guarantees better stability.

Figs. 9 and 10 show the injected reactive power and the PCC voltage behaviors, respectively under 0.99 VD conditions. If only conventional TVC is used, the WF can supply ~0.07 p.u. reactive power to meet the grid code requirements strictly, which results in a very small voltage enhancement from ~0.01 p.u. to ~0.081 p.u.. With the SFCL only, of course the stator voltage can achieve to ~0.12 p.u., but there is no reactive power

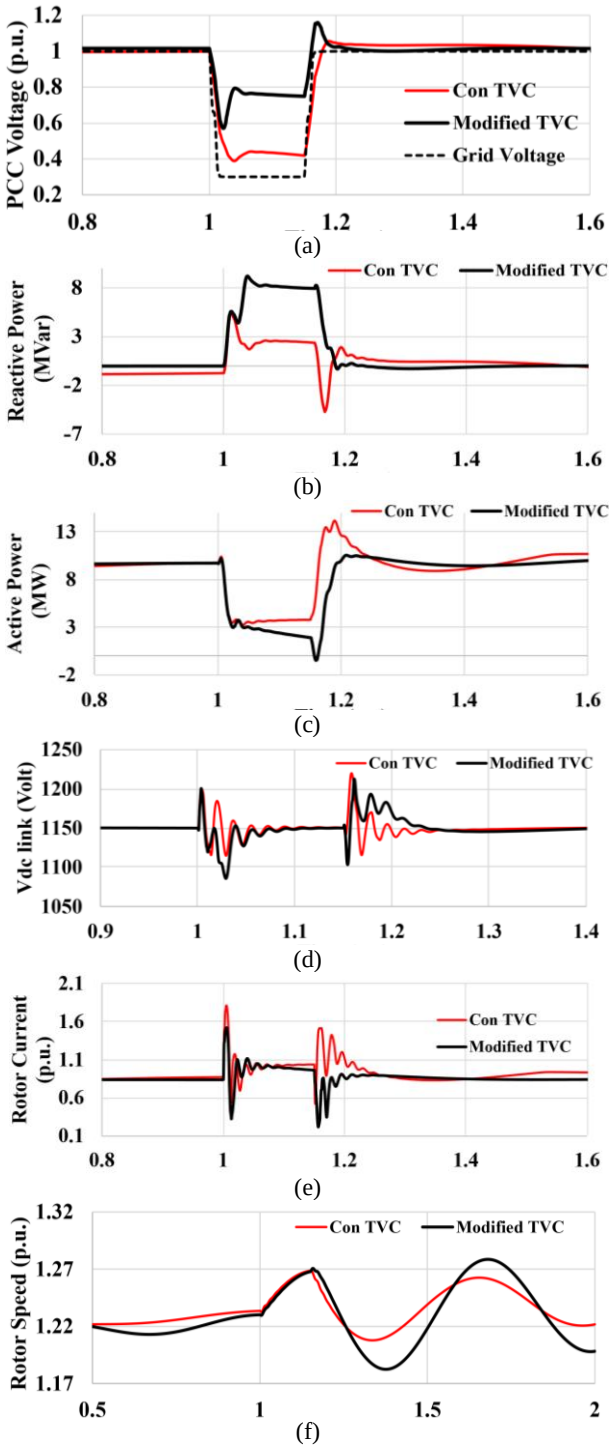

Fig. 2 a) PCC voltage, b) reactive power, c) active power, d) DC link voltage, e) rotor current, and f) rotor speed of DFIG-based WF during 70% VD.

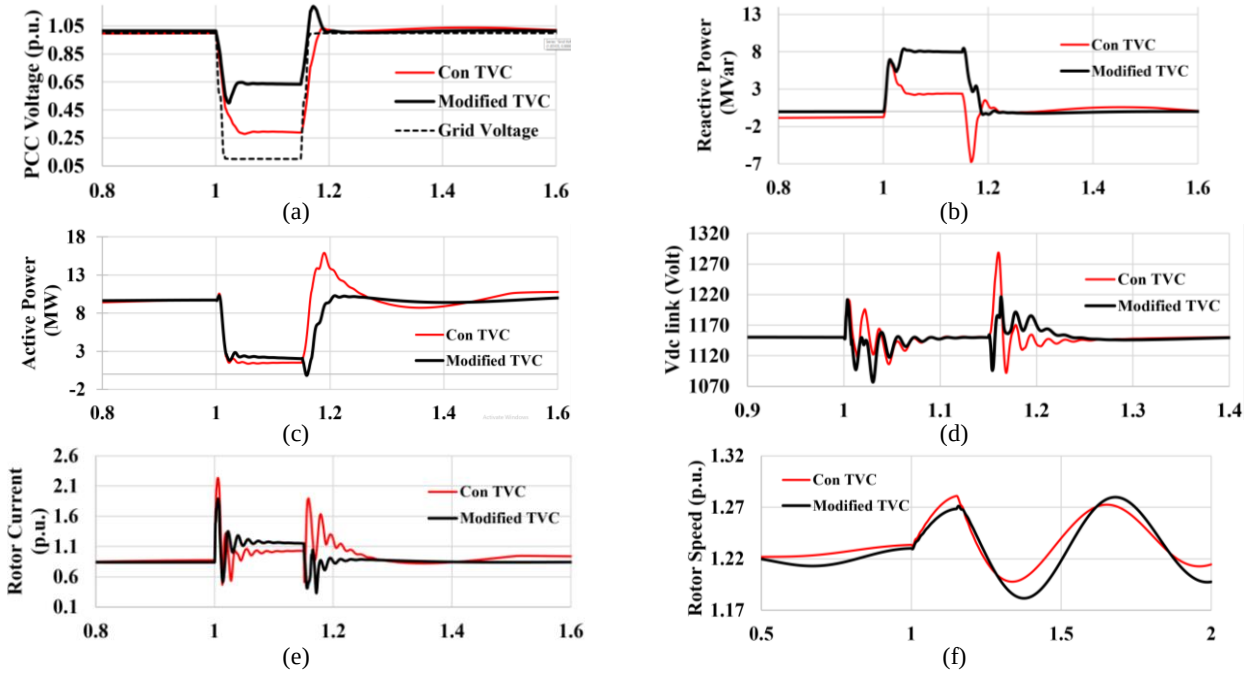

Fig. 8 a) PCC voltage, b) reactive power, c) active power, d) DC link voltage, e) rotor current, and f) rotor speed of DFIG-based WF during 90% VD.

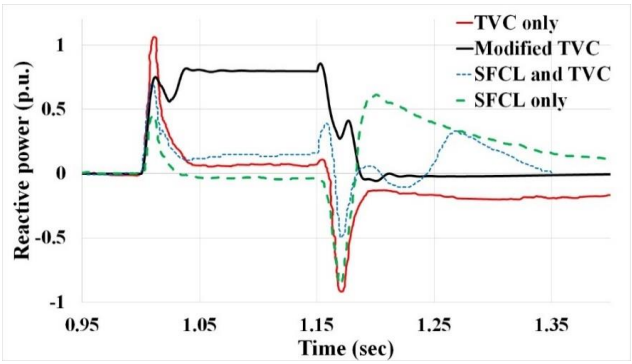

Fig. 9 Reactive power of DFIG-based WF under different approaches for 0.99 VD.

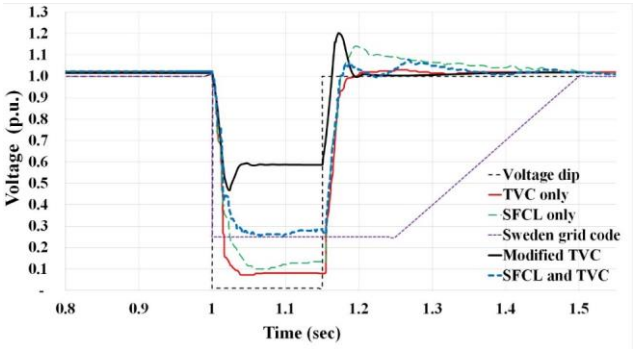

Fig. 10 Voltage of the PCC behavior under different approaches for 0.99 VD.

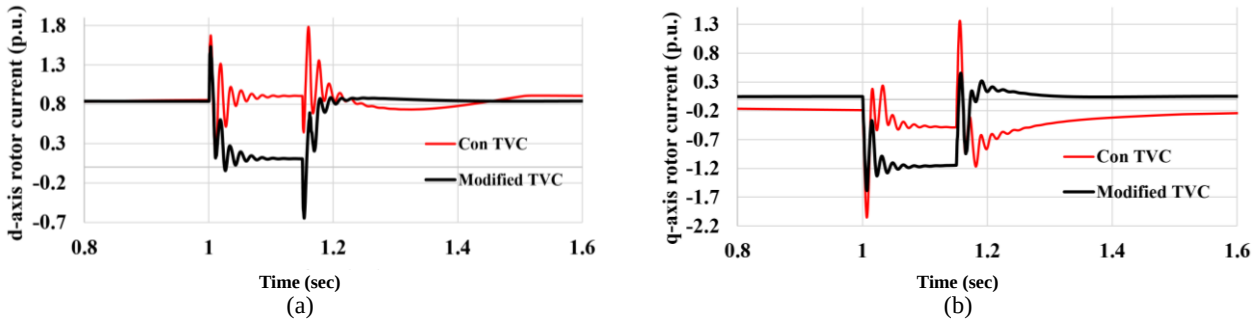

Fig. 11 a) Active and b) reactive rotor current of DFIG to 0.99 p.u. VD for scenarios A and B.

support. When the cooperative operation of the SFCL and TVC is applied, the DFIGs can output 0.147 p.u. reactive power and the minimum stator voltage is also improved to 0.27 p.u. for satisfying the Sweden grid code [2]. But, with employing the proposed modified TVC, the WF can inject 0.8 p.u. reactive power and the minimum stator voltage is also boosted to 0.582 p.u. to meet grid code requirement in many countries. Thus, the proposed approach improves the transient voltage stability. Moreover, as indicated in Figs. 11(a) and 11(b), it can be seen that the oscillations of the both rotor active and reactive currents (d-axis and q-axis, respectively) are significantly reduce when the modified TVC is applied. As illustrated and shown in these

figures, rotor reactive current rises to increase the reactive power during fault, while for decreasing the total rotor current, rotor active current decreases causing the reduction of the active power with using of the proposed approach. Depending on the results, it reveals that the transient voltage stability is well improved in the overall entire system by the use of modified TVC.

7 Conclusion

In this paper, a new controller-based strategy based on TVC is proposed for attenuating the side effects of a severe VD condition and improving transient voltage stability of grid-connected DFIG-based WF. In the proposed approach by changing both active and reactive power reference values, not only DC-link overvoltage and rotor overcurrent but also the PCC voltage can be properly controlled. In this proposed control strategy, a voltage dip index (VDI) is proposed suggested as a detection index to activate and deactivate the proposed control strategy (modified TVC). In this approach, by using vector control theory, the direct power control method is modified to adaptively change the reference values based on the severity of VD while avoiding rotor overcurrent increase. In the proposed modified TVC approach, the parameters of the PI controllers are tuned using the imperialist competitive algorithm (ICA). The main advantage of the proposed control method is its control-based nature which makes it easy for implementation into the grid without requirement for any additional extra devices, so the cost of implementation of extra device reduces and WF do not need ancillary devices. The simulation results show that for a severe VD condition, the modified TVC is able to decrease DC link overvoltage and rotor overcurrent while increasing transient voltage stability during severe VD condition in comparison with only the conventional TVC applies. The voltage improvement depends on the fault level of the terminal point and the amount of reactive power which can be injected into the grid by DFIG. For the case of 0.99% VD condition, the reduction of the DC link overvoltage and rotor overcurrent are good compared with the other method which demonstrates the ability of the modified TVC for improving transient voltage stability.

Appendix

Table A1 Induction machine parameters.

Rated power WF	9 MVA	Rotor voltage	1975
Stator voltage	575 V	Rotor leakage inductance	0.16 p.u.
Magnetization inductance generator	2.9 p.u.	Rotor resistance	0.016 p.u.
Stator leakage inductance	0.18 p.u.	Number of pair of poles	3
Stator resistance	0.023 p.u.	Slip	-0.2

Table A2 Line and grid parameters.

Grid	Line
S = 2500 MVA	R_{Line} = 0.1153 Ω/km
V_n = 120 kV	X_{Line} = 1.05e-3 Ω/km
R_{mu} = 0.1 p.u., X_{mu} = 1.0 p.u.	Line length = 50 km.
High voltage transformer	Medium voltage transformer
P_n = 47 MW	P_n = 10 MW
V_{n1}=120 kV, V_{n2} = 25 kV	V_{n1} = 25kV, V_{n2} = 690 V
R_1 = 0.08/30 p.u.	R_1 = 0.025/30 p.u.
X_1 = 0.08 p.u.	X_1 = 0.025 p.u.,
R_2 = 0.08/30 p.u.	R_2 = 0.025/30 p.u.
X_2 = 0.08 p.u.	X_2 = 0.025 p.u..

References

[1] H. E. Murdock, D. Gibb, T. André, F. Appavou, A. Brown, B. Epp, B. Kondev, A. McCrone, E. Musolino, L. Ranalder, and J. L. Sawin, "Renewables 2019: Global status report," *REN21 Secretariat*, 2019.

[2] Global wind Energy Council, "Global wind report 2018," 2019.

[3] H. Benbouhenni, "Sliding mode with neural network regulator for DFIG using two-level NPWM strategy," *Iranian Journal of Electrical and Electronic Engineering*, Vol. 15, No. 3, pp. 411–419, 2019.

[4] M. J. Abbasi and H. Yaghobi, "Loss of excitation detection in doubly fed induction generator by voltage and reactive power rate," *Iranian Journal of Electrical and Electronic Engineering*, Vol. 12, No. 4, pp. 270–280, Dec. 2016.

[5] R. Pour Ebrahim, S. Tohidi, and A. Younesi, "Sensorless model reference adaptive control of DFIG by using high frequency signal injection and fuzzy logic control," *Iranian Journal of Electrical and Electronic Engineering*, Vol. 14, No. 1, pp. 11–21, 2018.

[6] Y. K. Wu, T. C. Lee, T. Y. Hsieh, and W. M. Lin, "Impact on critical clearing time after integrating large-scale wind power into Taiwan power system," *Sustain. Energy Technol. Assessments*, Vol. 16, pp. 128–136, Aug. 2016.

[7] R. Ou, X. Y. Xiao, Z. C. Zou, Y. Zhang, and Y. H. Wang, "Cooperative control of SFCL and reactive power for improving the transient voltage stability of grid-connected wind farm with DFIGs," *IEEE Transactions on Applied Superconductivity*, Vol. 26, No. 7, pp. 1–6, Oct. 2016.

[8] W. Teng and Y. Meng, "Rotor-reference-current-oriented control strategy for low-voltage ride-through of DFIG," *IEEJ Transactions on Electrical and Electronic Engineering*, Vol. 13, No. 10, pp. 1421–1429, Oct. 2018.

[9] Z. Rafiee, M. Rafiee, and M. R. Aghamohammadi, "The voltage dip and doubly fed induction generator with considering uncertainty conditions," *Bulletin of Electrical Engineering and Informatics*, Vol. 9, No. 1, pp. 30–38, Feb. 2020.

[10] H. Shahbabaei Kartijkolaie, M. Radmehr, and M. Firouzi, "LVRT capability enhancement of DFIG-based wind farms by using capacitive DC reactor-type fault current limiter," *International Journal of Electrical Power & Energy Systems*, vol. 102, pp. 287–295, Nov. 2018.

[11] M. Rahimi, "Coordinated control of rotor and grid sides converters in DFIG based wind turbines for providing optimal reactive power support and voltage regulation," *Sustainable Energy Technologies and Assessments*, Vol. 20, pp. 47–57, Apr. 2017.

[12] M. K. Döşoğlu, "Enhancement of SDRU and RCC for low voltage ride through capability in DFIG based wind farm," *Electrical Engineering*, Vol. 99, No. 2, pp. 673–683, Jun. 2017.

[13] J. J. Justo, F. Mwasilu, and J. W. Jung, "Effective protection for doubly fed induction generator-based wind turbines under three-phase fault conditions," *Electrical Engineering*, Vol. 100, No. 2, pp. 543–556, Jun. 2018.

[14] M. G. Hemeida, H. Rezk, and M. M. Hamada, "A comprehensive comparison of STATCOM versus SVC-based fuzzy controller for stability improvement of wind farm connected to multi-machine power system," *Electrical Engineering*, Vol. 100, No. 2, pp. 935–951, Jun. 2018.

[15] A. Darvish Falehi and M. Rafiee, "Fault ride-through capability enhancement of DFIG-based wind turbine using novel dynamic voltage restorer based on two switches boost converter coupled with quinary multi-level inverter," *Energy Systems*, Vol. 9, No. 4, pp. 1071–1094, Sep. 2017.

[16] A. D. Falehi and M. Rafiee, "Enhancement of DFIG-wind turbine's LVRT capability using novel DVR based odd-nary cascaded asymmetric multi-level inverter," *Engineering Science and Technology, an International Journal*, Vol. 20, No. 3, pp. 805–824, Jun. 2017.

[17] A. H. M. A. Rahim and E. P. Nowicki, "Supercapacitor energy storage system for fault ride-through of a DFIG wind generation system," *Energy Conversion and Management*, Vol. 59, pp. 96–102, Jul. 2012.

[18] M. Wang, W. Xu, H. Jia, and X. Yu, "A novel method to optimize the active crowbar resistance for low voltage ride through operation of doubly-fed induction generator based on wind energy," in *IEEE International Symposium on Industrial Electronics*, pp. 957–962, 2012.

[19] A. Causebrook, D. J. Atkinson, and A. G. Jack, "Fault ride-through of large wind farms using series dynamic braking resistors (March 2007)," *IEEE Transactions on Power Systems*, Vol. 22, No. 3, pp. 966–975, Aug. 2007.

[20] M. Hasan Ali and A. A. Hussein, "Comparison among series compensators for transient stability enhancement of doubly fed induction generator based variable speed wind turbines," *IET Renewable Power Generation*, Vol. 10, No. 1, pp. 116–126, Jan. 2016.

[21] W. Guo, L. Xiao, S. Dai, X. Xu, Y. Li, and Y. Wang, "Evaluation of the performance of BTFCLs for enhancing LVRT capability of DFIG," *IEEE Transactions on Power Electronics*, Vol. 30, No. 7, pp. 3623–3637, Jul. 2015.

[22] S. B. Naderi, M. Negnevitsky, A. Jalilian, M. Tarafdar Hagh, and K. M. Muttaqi, "Low voltage ride-through enhancement of DFIG-based wind turbine using DC link switchable resistive type fault current limiter," *International Journal of Electrical Power & Energy Systems*, Vol. 86, pp. 104–119, Mar. 2017.

[23] Z. Rafiee, S. S. Najafi, M. Rafiee, M. R. Aghamohammadi, and M. Pourgholi, "Optimized control of coordinated series resistive limiter and SMES for improving LVRT using TVC in DFIG-base wind farm," *Physica C: Superconductivity and its Applications*, p. 1353607, Feb. 2020.

[24] P. M. Tripathi, S. S. Sahoo, and K. Chatterjee, "Enhancement of low-voltage ride through of wind energy conversion system using superconducting saturated core fault current limiter," *International Transactions on Electrical Energy Systems*, p. e2798, Dec. 2018.

[25] Z. C. Zou, J. C. Liao, Y. Lei, Z. L. Mu, and X. Y. Xiao, "Postfault LVRT Performance enhancement of DFIG using a stage-controlled SSFCL-RSDR," *IEEE Transactions on Applied Superconductivity*, Vol. 29, No. 2, pp. 1–6, Mar. 2019.

[26] H. Qingjun, S. Mucun, Z. Xudong, T. Li, X. Wei, and C. Jianqing, "A reverse current tracking based LVRT strategy for doubly fed induction generator (DFIG)," in *IECON 2013-39th Annual Conference of the IEEE Industrial Electronics Society*, pp. 7295–7300, 2013.

[27] J. J. Justo, F. Mwasilu, and J. W. Jung, "Enhanced crowbarless FRT strategy for DFIG based wind turbines under three-phase voltage dip," *Electric Power Systems Research*, Vol. 142, pp. 215–226, Jan. 2017.

[28] H. Ahmadi, A. Rajaei, M. Nayeripour, and M. Ghani, "A hybrid control method to improve LVRT and FRT in DFIG by Using the multi-objective algorithm of Krill and the fuzzy logic," *Iranian Journal of Electrical and Electronic Engineering*, Vol. 14, No. 4, pp. 330–341, Dec. 2018.

[29] R. Ghazi and A. Khajeh, "GA-Based Optimal LQR controller to improve LVRT capability of DFIG wind turbines," *Iranian Journal of Electrical and Electronic Engineering*, Vol. 9, No. 3, pp. 167–176, 2013.

[30] D. Xie, Z. Xu, L. Yang, J. Ostergaard, Y. Xue, and K. P. Wong, "A comprehensive LVRT control strategy for DFIG Wind turbines with enhanced reactive power support," *IEEE Transactions on Power Systems*, Vol. 28, No. 3, pp. 3302–3310, Aug. 2013.

[31] M. Ahmed, M. EL-Shimy, and M. A. Badr, "Advanced modeling and analysis of the loading capability limits of doubly-fed induction generators," *Sustainable Energy Technologies and Assessments*, Vol. 7, pp. 79–90, Sep. 2014.

[32] S. Chondrogiannis and M. Barnes, "Specification of rotor side voltage source inverter of a doubly-fed induction generator for achieving ride-through capability," *IET Renewable Power Generation*, Vol. 2, no. 3, pp. 139–150, Sep. 2008.

[33] S. Xiao, G. Yang, H. Zhou, and H. Geng, "An LVRT Control strategy based on flux linkage tracking for DFIG-based WECS," *IEEE Transactions on Industrial Electronics*, Vol. 60, No. 7, pp. 2820–2832, Jul. 2013.

[34] E. Heydari, M. Rafiee, and M. Pichan, "Fuzzy-genetic algorithm-based direct power control strategy for DFIG," *Iranian Journal of Electrical and Electronic Engineering*, Vol. 14, No. 4, pp. 353–361, Dec. 2018.

[35] L. Yang, Z. Xu, J. Ostergaard, Z. Y. Dong, and K. P. Wong, "Advanced control strategy of DFIG wind turbines for power system fault ride through," *IEEE Transactions on Power Systems*, Vol. 27, No. 2, pp. 713–722, May 2012.

[36] E. Atashpaz-Gargari and C. Lucas, "Imperialist competitive algorithm: An algorithm for optimization inspired by imperialistic competition," in *IEEE Congress on Evolutionary Computation*, pp. 4661–4667, 2007.

[37] Z. Rafiee, S. Ganjefar, and A. Fattahi, "A new PSS tuning technique using ICA and PSO methods with the fourier transform," in *18th Iranian Conference on Electrical Engineering* (ICEE 2010), pp. 806–811, 2010.

[38] Z. Rafiee, A. F. Meyabadi, and H. Heydari, "PSS parameters values finding using SMVSDFT objective function and a new technique for multi-objective function in a multi-machine power system," *International Journal of Power and Energy Conversion*, Vol. 6, No. 3, p. 252, 2015.

[39] Z. Rafiee and A. F. Meyabadi, "Optimal design of power system stabiliser using a new cost function and PSO algorithm," *International Journal of Power and Energy Conversion*, Vol. 3, No. 3-4, p. 253, 2012.

Z. Rafiee received her B.Sc. degree in Power Electricity Engineering from the Department of Electrical Engineering, Bu Ali Sina University, Hamadan Iran, in 2006 and an M.Sc. degree in Power Electricity Engineering from the Department of Electrical Engineering, Bu Ali Sina University, Hamadan Iran, in 2010. She studies Ph.D. in Electrical Engineering in Shahid Beheshti University. Her research interests are in stability in power system, protection of network, optimization control algorithms, power system stabilizer and, distributed generation, application of neural network and fuzzy logic in electricity.

M. Raftee was born in Iran in 1967. He received his B.Sc. degree from the Sharif University of Technology in 1981, M.Sc. degree from KNT University of Technology in 1996 and Ph.D. Degree from Iran University of Science and Technology (IUST) in 2006, all in Electrical Engineering. He is currently Assistant Professor in Shahid Beheshti University (SBU) and his current research interests include modeling and analysis of distributed generation and renewable energy.

M. R. Aghamohammadi was born in Iran on August 5, 1955. He received his B.Sc. degree from Sharif University of Technology 1981, M.Sc. degree from Manchester University (UMIST) in 1984 and his Ph.D. from Tohoku University, Japan in 1994. He is an Associate Professor of the Electrical Engineering Department and Head of Iran Dynamic Research Center. His research interest includes application of intelligent techniques and non-model based approaches for dynamic security assessment and enhancement of power systems.